A Kr−BrH Global Minimum Structure Determined on the Basis of Potential Morphing†

Z. Wang, R. R. Lucchese,* and J. W. Bevan

Chemistry Department, Texas A&M University, College Station, Texas 77843-3255

Received: September 1, 2003; In Final Form: January 29, 2004

The ν_1, $\nu_1 + \nu_2^1$, and $\nu_1 + 2\nu_2^0$ rovibrational spectra of ^{84}Kr:H^{79}Br and ^{84}Kr:H^{81}Br are reported using high-frequency wavelength modulation near-infrared diode-laser continuous-wave (cw) supersonic-jet spectroscopy. This information has been combined with previously recorded results from a ground-state microwave analysis and used to determine a scaled and shifted morphed potential that is based on the transformation of an ab initio potential in a nonlinear least-squares fit to the available experimental data. The morphed potential is consistent with a collinear Kr−BrH global minimum structure with $R_{cm} = 3.88$ Å that is 23 ± 3 cm^{-1} more stable than the minimum associated with the collinear Kr−HBr isomeric form, which has $R_{cm} = 4.27$ Å. Thus, the Kr:HBr system has a ground-vibrational-state isomeric structure that differs from the global minimum energy structure, a result that is similar to that found in the Ar:HBr dimer.

Introduction

In a recent set of investigations that involved potential morphing of the dimer Ar:HBr, it has been proposed that the arrangement of atoms in the ground-vibrational-state isomeric structure of the dimer (Ar−HBr) is different from its collinear isomeric Ar−BrH global minimum energy structure.[1,2] Thus, this complex is an example of a restricted number of molecular species for which the isomeric structure in the ground state has been demonstrated to be different from that at its global minimum. This structural change has been attributed to zero-point energy effects that are associated with anharmonic large amplitude vibrations in weakly bound molecular species. In particular, in the Ar:HBr complex, this observation can be reconciled with zero-point effects that are associated with the shallower portion of the potential minimum characteristic of the hydrogen-bound (HB) isomer, relative to that of the van der Waals (vdW) Ar−BrH isomeric form.[2] Similar characteristics have been claimed for the molecular complexes He:Cl_2 and $(H_2O)_6$.[3,4] The question arises as to whether the number of molecular species that have such structural characteristics are restricted and represent curiosities, or are more ubiquitous in nature. More specifically, will this effect be observed if the more easily polarizable Kr atom is substituted for the Ar atom in the Ar:HBr dimer?

Kr:HBr is a complex that has been the subject of previous microwave investigations under the isolated conditions of a pulsed supersonic-jet expansion, and also several theoretical calculations.[5−8] The initial pulsed-nozzle Fourier transform (FT)−microwave spectroscopic study[5] definitively established an R_0 value of 4.2573 Å with an angle $\cos^{-1}(\langle\cos^2\theta\rangle^{1/2}) = 38.03°$ (defined as ∠Kr−(center of mass of BrH)−H). The consensus of these studies has been that the ground-state structure is the isomeric form Kr−HBr, and that the global minimum has a similar collinear isomeric form. In an extensive theoretical investigation, Hutson[6] determined a value of $R_m(0°) = 4.3311$ Å from his H4 potential, corresponding to the Kr−HBr atomic arrangement. The complex has subsequently been the subject of further theoretical consideration in the predictions of Bulanin and Bulychev[7] and an application of Watson's method[9] for structural determination in weakly bound complexes by Kisiel.[8] However, we know of no further experimental studies that would give additional perspectives on these studies.

In this study, we use the potential morphing method to obtain an interaction potential for Kr:HBr. Potential morphing is a procedure for combining a variety of experimental data with theoretical models to obtain such potentials.[10,11] The basic idea is to compute a complete interaction potential for the system at some level of theory. The potential then provides a functional form that can be used to represent the true interaction potential. Parameters are introduced to modify this potential through scaling, shifting, and dilation that combine to form what is called the morphing transformation. The parameters are determined in a nonlinear least-squares fit of quantities predicted from the morphed potential to the corresponding available experimental data. In the region of the potential interrogated by the experiments, the potential can be accurately determined.[12] In the other regions of the interaction potential, the ab initio potential provides a means of interpolation and extrapolation. This approach has been previously used to determine two- and three-dimensional intermolecular potentials such as that studied here.[1,2,10−14] We also note that one can start with potentials computed at somewhat different levels of theory and yield morphed potentials of very similar quality.[10]

In this work, we now report the analysis of the ν_1, $\nu_1 + \nu_2^1$, and $\nu_1 + 2\nu_2^0$ rovibrational spectra of the ^{84}Kr:H^{79}Br and ^{84}Kr:H^{81}Br isotopomers, recorded using high-frequency wavelength modulation near-infrared diode-laser continuous-wave (cw) supersonic-jet spectroscopy.[15,16] These data are then combined with the previously recorded ground-state microwave data[5] to determine a morphed potential.[1,10,11] We then compare the morphed potential of Kr:HBr with the results of previous investigations of the complex[5−8] and with the potentials of the related dimers Ar:HX [X = F, Cl, Br, I][17−19] and, in particular, the morphed potentials for Ar:HBr.[1,2]

* Author to whom correspondence should be addressed. E-mail address: lucchese@mail.chem.tamu.edu.

† Part of the special issue "Fritz Schaefer Festschrift".

10.1021/jp036603p CCC: $27.50
Published on Web 03/25/2004

Experimental Section

The supersonic-jet spectra of the ν_1, $\nu_1 + 2\nu_2^0$, and $\nu_1 + \nu_2^1$ bands of Kr:HBr were recorded using a tunable infrared diode-laser cw supersonic slit-jet spectrometer with an InSb detector. The spectrometer has been discussed in detail elsewhere.[15,16] Briefly, a II−VI lead salt diode laser was acquired from Laser Analytics, Inc., Boston, MA, and was centered at 3.929 μm but could be tuned to cover the frequency range of 2537−2612 cm^{-1} in single frequency. This spectrometer was capable of operating with an applied source modulation up to 500 kHz, up to 1 MHz with second-derivative detection and giving an instrumental resolution of 30 MHz or less. The spectrometer has been shown to have an ultimate sensitivity that is consistent with an equivalent minimum absorbance of 2 parts in 10^7 or better. The supersonic-jet expansion was formed from a gaseous reservoir that typically consisted of 1% HBr in krypton as the carrier gas with a reservoir pressure that was sustained at 2.0×10^5 Pa. The supersonic-jet expansion was formed through a 12.7-cm-long slit with a width of 25 μm and all spectra recorded with a single pass of the laser beam through the cw slit-jet expansion.[19] The krypton gas consists of naturally occurring ^{84}Kr, ^{86}Kr, ^{82}Kr, ^{83}Kr, ^{79}Kr, and ^{78}Kr isotopes with respective abundances of 56.90%, 17.37%, 11.56%, 11.55%, 2.27%, and 0.35%.[20] Bromine occurs with the corresponding abundances of ^{79}Br (50.537%) and ^{81}Br (49.463%). The observed spectrum of Kr:HBr thus consists of a complex isotopic distribution of isotopomers that are characteristic of these different isotopic distributions. For the purposes of the current combined experimental and theoretical investigation, we report the assignment of the ^{84}Kr:H^{79}Br and ^{84}Kr:H^{81}Br isotopomers, which represent the two most abundant isotopic species and dominate the observed spectra.

The transition frequencies in the spectrum of Kr:HBr complex were calibrated to an estimated absolute accuracy of 0.001 cm^{-1} or better, using standard frequencies of a simultaneously recorded spectrum of N_2O.[21]

Theoretical Calculations

We have also studied the Kr−H^{79}Br complex using ab initio methods combined with potential morphing, so that we can extract a global potential energy surface.[11] To study this system, we have computed the interaction energy on a three-dimensional grid of points. The interaction energy was computed at six values of the H−Br bond length with the values of r evenly spaced, starting with $r = 1.2144$ Å and ending with $r = 1.7144$ Å. Note that this includes the equilibrium value[22] of $r_e = 1.4144$ Å. Fifteen values of the distance between the Kr and Br atoms are considered: $R = 2.0$, 3.0, 3.4, 3.6, 3.8, 4.0, 4.2, 4.4, 4.6, 4.8, 5.0, 5.2, 6.0, 8.0, and 10.0 Å. In addition, 10 evenly spaced values of the angle θ (H−Br−Kr) were considered, starting at $\theta = 0°$ and ending with $\theta = 180°$. Thus, the total number of points calculated was $M = 900$. At each geometry, the energy was computed using second-order Møller−Plesset perturbation theory (MP2), using the triple-ζ form of the augmented correlation consistent basis sets (aug-cc-pVnZ) of Dunning and co-workers.[23,24] Except where noted, all electronic structure calculations did not correlate the 1s, 2s, 2p, 3s, or 3p orbitals on the Kr and Br atoms. The interaction energies were then corrected for the basis set superposition error (BSSE) using the counterpoise (CP) method of Boys and Bernardi.[25] Electronic structure calculations were performed using the Gaussian[26] and MOLPRO[27] electronic structure packages.

The computed interaction energies were fitted to an analytical form, using a three-dimensional interpolation function that was based on the Hilbert space reproducing kernel (HSRK) of Ho and Rabitz.[28] The approach is very similar to the method we used in our earlier study of the three-dimensional potential of Ar:HBr.[1] In that earlier study, we used a smoothed version of the HSRK. In those potentials, we found weak oscillations in the potential that resulted from the smoothing. Thus, in the current application, we have removed the smoothing, i.e., set the switching range Δx to zero.

The rovibrational states were then computed using the variational method that was previously described in detail.[1,12,29,30] In this approach, the H−Br stretching motion is adiabatically separated from the bending and stretching motion of the complex. Thus, at each value of R and θ, the energy of the H−Br(υ_1) stretching state $E_{\upsilon_1}(R,\theta)$ is determined. This energy then becomes the potential for the determination of the bending and stretching motion of the complex. The intermolecular rovibrational wave function is computed using a space-fixed frame with the radial function expanded in a distributed Gaussian basis set and the angular function expanded in a coupled angular basis set. The distributed Gaussian basis set consisted of 50 functions evenly distributed from $R = 3$ Å to $R = 7$ Å. The angular basis set contained an expansion of the rotational wave function of the HBr monomer, using states up to $j_{max} = 14$. All possible end-over-end rotational states were included that were consistent with this value of j_{max} and the value of the total angular momentum of a given state. The rovibrational states are computed in two steps. First, a vibrational self-consistent field (VSCF) calculation is performed in which the angular state is computed in an angular potential obtained from the full intermolecular potential by averaging over the ground radial vibrational state, and the radial state is obtained from a one-dimensional vibrational calculation where the potential is obtained from the full intermolecular potential by averaging over the bending state. The VSCF equations are solved iteratively. The converged VSCF bending and stretching wave functions are then combined in a direct product basis set, which is used in a vibrational configuration interaction (VCI) calculation for the final rovibrational states. In the morphing procedure discussed below, the derivatives of the rovibrational eigenvalues with respect to the morphing parameters are used. These derivatives are computed using the Hellmann−Feynman theorem. The rotational constants used for the diatomic molecules in the complex were taken to be the same as for the isolated molecules: 8.351061 cm^{-1} for^{31} H^{79}Br($\upsilon = 0$), 8.119 cm^{-1} for^{32} H^{79}Br($\upsilon = 1$), and 4.2481936 cm^{-1} for^{31} D^{79}Br($\upsilon = 0$).

The ab initio potential, $V_{\text{ab initio}}(R,\theta,r)$, is morphed using the transformation

$$V_{\text{morphed}}(R,\theta,r) = S_1(\theta,r)V_{\text{ab initio}}[S_2(\theta,r)(R - R_F) + (1 + S_3(\theta,r))R_F,\theta,r] \quad (1)$$

where

$$S_\alpha(\theta,r) = \sum_{i,j} C_{\alpha,i,j} P_i(\cos\theta)\left[1 - \exp\left(-\beta\frac{r - r_e}{r_e}\right)\right]^j \quad (2)$$

We note that all of the morphing parameters $C_{\alpha,i,j}$ are numbers without units. In the present study, R_F was assumed to be 4.0 Å and β was assumed to be 1.0. The values of the morphing parameters were obtained by a regularized nonlinear least-

squares optimization. In the regularized procedure, the function that is minimized is

$$F(C_{\alpha,i,j},\gamma) = \sum_{k=1}^{M}\left[\frac{O_k^{\text{expt}} - O_k^{\text{calc}}(C_{\alpha,i,j})}{\sigma_k}\right]^2 + \gamma^2\sum_{\alpha,i,j}(C_{\alpha,i,j} - C_{\alpha,i,j}^0)^2 \quad (3)$$

where O_k^{expt} are the experimentally observed quantities, O_k^{calc} are the corresponding calculated quantities, γ is the regularization parameter, σ_k are the uncertainties in either the observed or computed values, and the $C_{\alpha,i,j}^0$ are the values of the morphing parameters that correspond to no morphing (i.e., $C_{1,0,0}^0 = 1, C_{2,0,0}^0 = 1$, and all others are zero). We note that all calculated quantities O_k^{calc} are obtained by finite difference, as described in our earlier study.[1] Minimizing F then yields a potential that simultaneously improves the agreement between the experimental and calculated observables and keeps the morphed potential close to the original ab initio potential. The quality of the fit of the experimental data can then be characterized by the root-mean-square deviation from the experimental data:

$$G(\gamma) = \left\{\frac{1}{M}\sum_{k=1}^{M}\left[\frac{O_k^{\text{expt}} - O_k^{\text{calc}}(C_{\alpha,i,j})}{\sigma_k}\right]^2\right\}^{1/2} \quad (4)$$

In eq 4, the value of G is dependent on the value of γ because the morphing parameters $C_{\alpha,i,j}$ are dependent implicitly on γ through the minimization of F that is given in eq 3. Note that $G(\gamma = \infty)$ is the deviation from the experimental data of the observables predicted from the ab initio potential energy surface (i.e., the unmorphed surface).

There is a direct connection between the type of available experimental data and the morphing parameters that can be determined. Rotation constants are most sensitive to the $C_{3,i,j}$ morphing parameters, which shift the potential. Distortion constants are sensitive to the curvature of the potential in the radial direction, which is controlled by the overall scaling parameters $C_{1,i,j}$ and the radial dilation parameters $C_{2,i,j}$. The values of $\langle P_2(\cos\theta)\rangle$, the energy difference between the Kr−HBr and Kr−BrH vibrational states, and the frequency of the bending mode are sensitive to the overall scaling parameters $C_{1,i,j}$.

We have also estimated the uncertainty in the morphed potential by considering the sensitivity of the values of the potential to the quality of the fit. Using the same approach as that in our previous work,[1] the computed uncertainties represent the root-mean-square difference in the potential between the optimized value and the value of the potential where the parameters are on the boundary of the confidence region with $\Delta\chi^2 = \chi^2_{\text{min}}$.[33] The values of the potential used in the uncertainty estimate were relative to the value at the minimum in the HB structure. Thus, we have fixed the uncertainty at the HB structure to be zero.

Results

A segment of the $P(11)$ to $R(2)$ branches of the rovibrationally resolved spectrum of ν_1 in the ^{84}Kr:H^{79}Br isotopomer, and the $P(3)$ to $R(9)$ branches of ν_1 of the ^{84}Kr:H^{81}Br isotopomer, are shown in Figure 1. The quadrupole substructure associated with these transitions has collapsed and is not resolved in the presented spectrum. It is pertinent to note that this spectrum is relatively congested, because of the presence of different naturally occurring isotopomers of Kr and Br. This latter effect, and the limited populations in the supersonic expansion that are due to the relatively larger frequencies (>25 cm^{-1}) of the low-frequency intermolecular states in this complex, are factors that combine so that it was not possible for us to assign hot bands associated with low-frequency intermolecular vibrations in Kr:HBr. This spectrum lacks a $Q(J)$ branch and has characteristics of a $\Sigma \leftarrow \Sigma$ band with pronounced $P(J)$ and $R(J)$ transitions that can readily be assigned on the basis of comparison with combination differences generated from ground-state molecular parameters determined using pulsed-nozzle FT microwave spectroscopy. The observed $P(J)$ and $R(J)$ transitions were fitted using the expression

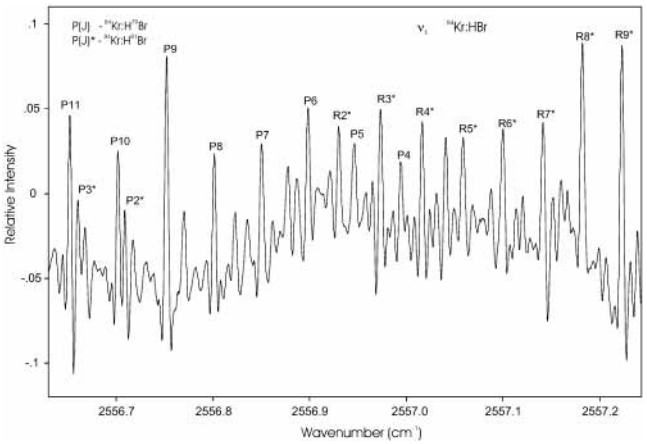

Figure 1. Segment of the assigned $P(J)$ and $R(J)$ branch transitions of the H−Br(ν_1) stretching fundamental in the ^{84}Kr:H^{79}Br and ^{84}Kr:H^{81}Br isotopomers.

$$\nu = \nu_0 + [B'J'(J'+1) - D_J'J'^2(J'+1)^2] - [B''J''(J''+1) - D_J''J''^2(J''+1)^2] \quad (5)$$

The rotational assignment can be rapidly confirmed by determining lower-state-combination differences for these transitions and comparing them with the corresponding values based on the microwave analyses of the ^{84}Kr−H^{79}Br and ^{84}Kr−H^{81}Br isotopomers reported previously.[5] The spectra of the isotopomers were recorded from 2553 cm^{-1} to 2560 cm^{-1} and transition frequencies associated with $P(4)$ to $P(59)$, $R(2)$ to $R(53)$ for the Kr−H^{79}Br isotopomer, and with $P(2)$ to $P(53)$, $R(2)$ to $R(38)$ for the Kr−H^{81}Br isotopomer were recorded and their frequencies measured. In fitting these transitions to the expression given in eq 5, the ground state is fixed to the previously and precisely determined values of B_0 and D_J^0 that are available from pulsed-nozzle FT microwave spectroscopy. The resulting fits are given in Table 1. The quoted uncertainties of all experimentally determined molecular parameters given in this paper represent statistical uncertainties of the fitted data. Absolute frequency accuracies of the band origins are estimated[21] to be ± 0.001 cm^{-1}.

Interestingly, the ν_1 band origins in the ^{84}Kr:H^{79}Br and ^{84}Kr:H^{81}Br isotopomers are red-shifted by 1.5491(13) and 1.5491(13) cm^{-1} from the band origins of the respective H^{79}Br and H^{81}Br monomeric isotopomers. This indicates that the excited-vibrational-state dissociation energy of this complex is slightly stronger than that of the corresponding ground-state complex. A similar effect has been observed for the ^{40}Ar−^{79}BrH and ^{40}Ar−^{81}BrH isotopomers, where the corresponding red shifts were 1.46111(30) and 1.46174(29) cm^{-1}, respectively.[1] In contrast, the corresponding Ar−HBr complexes were blue-

TABLE 1: Rovibrational Constants Obtained from the Infrared Analysis of Kr:HBr

constant	$(00^00)^a$	(10^00)	$(11^{1e}0)$	(12^00)
		^{84}Kr:H^{79}Br Isotopomer		
ν_v (cm^{-1}) ^{b}		2557.17899(6)	2589.73736(8)	2593.00129(9)
B_v ($\times 10^{-2}$ cm^{-1})	2.28234	2.25873(2)	2.34941(2)	2.51351(3)
D_J^v ($\times 10^{-7}$ cm^{-1})	0.866366	0.8631(2)	0.5673(13)	2.139(2)
σ (cm^{-1})		0.0002	0.0003	0.0003
		^{84}Kr:H^{81}Br Isotopomer		
ν_v (cm^{-1})^b		2556.79705(8)	2589.35427(10)	2592.50450(7)
B_v ($\times 10^{-2}$ cm^{-1})	2.25364	2.23036(3)	2.32031(2)	2.48357(2)
D_J^v ($\times 10^{-7}$ cm^{-1})	0.842783	0.8377(38)	0.5864(10)	2.101(2)
σ (cm^{-1})		0.0003	0.0004	0.0002

^{a} Microwave data from ref 5. ^{b} Fitted band origin frequency uncertainty; absolute accuracy is ± 0.001 cm^{-1}.

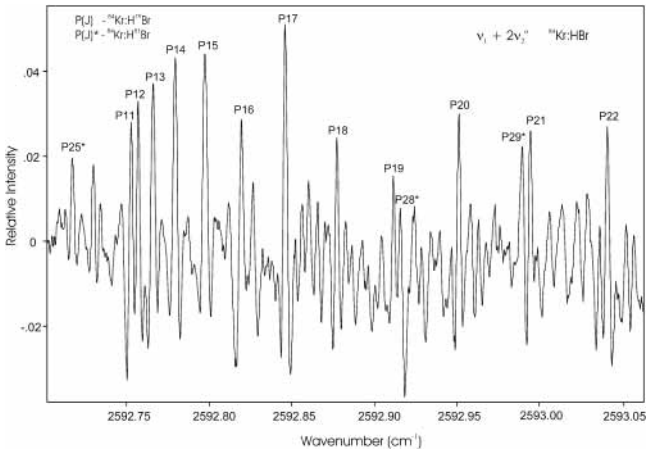

Figure 2. Partial scan recorded for the $P(J)$ branches of $\nu_1 + 2\nu_2^0$ in ^{84}Kr:H^{79}Br and ^{84}Kr:H^{81}Br, illustrating the prominent $P(J)$ head associated with the ^{84}Kr:H^{79}Br isotopomer. Only high $P(J)$ lines are labeled following the turn-around frequency.

shifted 0.33665(11) and 0.33970(12) cm^{-1} for the ^{79}Br and ^{81}Br isotopomers, respectively, with a corresponding decrease of the dissociation energy of the isotopomers in the excited vibrational states.[34]

A segment of the $P(J)$ branch that corresponds to the $\nu_1 + 2\nu_2^0$ vibrational band from $P(11)$ to $P(22)$ in the ^{84}Kr:H^{79}Br isotopomer is shown in Figure 2. Transitions from $P(4)$ to $P(42)$ and from $R(9)$ to $R(23)$ for the Kr:H^{79}Br isotopomer, and from $P(11)$ to $P(44)$ and from $R(3)$ to $R(19)$ for the ^{84}Kr:H^{81}Br isotopomer, were recorded and measured. Such spectra are also characteristic of $\Sigma-\Sigma$ vibrational bands and were similarly fitted to the ν_1 bands using the expression in eq 5. The ground-state constants are fixed at their ground-state values, as derived from microwave pulsed-nozzle FT microwave spectroscopy, and resulting fits are also given in Table 1.

Figure 3 shows a segment of the of the $\nu_1 + \nu_2^1$ band illustrating transitions from $R(12)$ to $R(18)$ for the ^{84}Kr:H^{79}Br isotopomer, and from $R(18)$ to $R(23)$ for the ^{84}Kr:H^{81}Br isopotomer. Such spectra were characteristic of a $\Pi-\Sigma$ transition with an intense $Q(J)$ branch and prominent $P(J)$ and $R(J)$ branches. Transitions from $P(4)$ to $P(27)$ and from $R(1)$ to $R(45)$ were recorded for the Kr−H^{79}Br isotopomer, and from $P(3)$ to $P(20)$ and from $R(1)$ to $R(52)$ for the Kr−H^{81}Br isotopomer. The spectra were fitted with an expression that was similar to eq 5, but with the addition of the excited-state terms to include the vibrational angular momentum quantum number (l). The results of the fits are also given in Table 1.

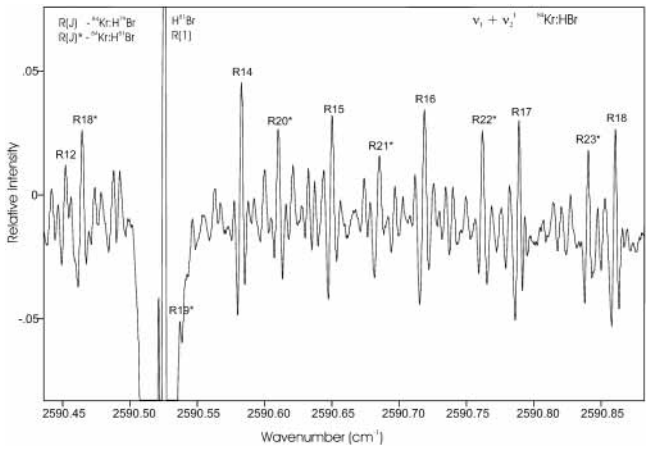

Figure 3. Segment of the assigned $R(J)$ branch of the combination band $\nu_1 + \nu_2^1$ associated with the ^{84}Kr:H^{79}Br and ^{84}Kr:H^{81}Br isotopomers; the intense and saturated transition is that assigned to the $R(1)$ transition of the H^{81}Br monomeric isotopomer.

TABLE 2: Value of the Optimized Morphing Parameters and Statistical Uncertainties

(α,i,j)	$C_{\alpha,i,j}$	$C^0_{\alpha,i,j}$	σ
(1,0,0)	(1.0)	1.0	not optimized
(1,1,0)	0.220	0.0	0.011
(1,2,0)	−0.179	0.0	0.010
(1,3,0)	−0.229	0.0	0.017
(1,4,0)	0.291	0.0	0.031
(1,0,1)	−0.309	0.0	0.037
(2,0,0)	1.389	1.0	0.019
(2,1,0)	−0.457	0.0	0.020
(3,0,0)	0.0125	0.0	0.0011
(3,1,0)	−0.0044	0.0	0.0019
(3,0,1)	−0.098	0.0	0.014

We then morphed the ab initio potential as discussed previously[1] by combining the rovibrational data obtained in this study and the microwave data of Keenan et al.[5] As discussed previously, this is a nonlinear least-squares fit. Thus, there is always the possibility that a given set of parameters may not yield the globally best fit and that there are fits of similar quality that have somewhat differing values of the parameters or differing choices of morphing parameters. For any given fit, it is possible to add more morphing parameters that would improve the fit. However, as more parameters are added to the morphing transformation, the parameters become highly correlated, which leads to large statistical uncertainties in the optimized parameters and large uncertainties in the resulting morphed potential. Our goal was to find a set of morphing parameters that yielded a good fit of the experimental spectroscopic constants and had statistically significant values of the morphing parameters. For the purposes of this study, we searched for a set of parameters where the statistical uncertainty of each parameter was less than half the value of the parameter. The morphing parameters were obtained using a three-stage procedure. First, we fitted the experimental data for the energy differences, $\langle P_2(\cos\theta)\rangle$, and rotational constants using the parameters that scale the depth of the potential ($C_{1,i,j}$) and shift the potential in the radial direction ($C_{3,i,j}$). In the second stage, we fit all of the data, including the distortion constants. In the final stage, we verified that additional morphing parameters would not be determined with statistical significance. In particular, we found that the parameters $C_{1,5,0}$, $C_{2,2,0}$, and $C_{3,2,0}$ could not be determined with statistical significance. In Table 2, we give the final morphing parameters that yielded the best fit of the experimental data. Note that we have not optimized the value of $C_{1,0,0}$, because

TABLE 3: Correlation Matrix of the Morphing Parameters ($C_{\alpha,i,j}$)

($\alpha.i,j$)	(1,1,0)	(1,2,0)	(1,3,0)	(1,4,0)	(1,0,1)	(2,0,0)	(2,1,0)	(3,0,0)	(3,1,0)	(3,0,1)
(1,1,0)	1.00									
(1,2,0)	−0.93	1.00								
(1,3,0)	−0.99	0.88	1.00							
(1,4,0)	0.98	−0.98	−0.95	1.00						
(1,0,1)	−0.10	0.23	0.09	−0.17	1.00					
(2,0,0)	−0.21	0.40	0.08	−0.26	0.40	1.00				
(2,1,0)	−0.16	−0.07	0.29	−0.09	−0.26	−0.90	1.00			
(3,0,0)	−0.57	0.61	0.54	−0.57	0.73	0.45	−0.17	1.00		
(3,1,0)	0.87	−0.88	−0.81	0.86	−0.36	−0.48	0.11	−0.83	1.00	
(3,0,1)	−0.20	0.09	0.19	−0.14	−0.95	−0.27	0.24	−0.55	0.08	1.00

TABLE 4: Predicted Spectroscopic Constants from $V_{\text{ab initio}} = V_{\text{morphed}}$ ($\gamma = \infty$) and V_{morphed} ($\gamma = 10$)[a]

			Experiment		Uncertainty	
	$V_{\text{ab initio}}$	V_{morphed}	value	reference(s)	value	note[c]
^{84}Kr−H^{79}Br(00^00) B_0 ($\times 10^{-2}$ cm^{-1})	2.236	2.285	2.282	Keenan et al.[5]	0.002	approximation
^{84}Kr−H^{79}Br(00^00) D_J ($\times 10^{-7}$ cm^{-1})	0.666	0.809	0.866	Keenan et al.[5]	0.01	systematic
^{84}Kr−H^{79}Br(00^00) $\langle P_2(\cos\theta)\rangle$	0.551	0.432	0.428	Keenan et al.[5]	0.01	systematic
^{84}Kr−H^{79}Br(00^00) D_θ ($\times 10^{-6}$)	4.1	13.1	14.2	Keenan et al.[5]	0.5	statistical
^{84}Kr−D^{79}Br(00^00) B_0 ($\times 10^{-2}$ cm^{-1})	2.221	2.253	2.254	Keenan et al.[5]	0.002	approximation
^{84}Kr−D^{79}Br(00^00) D_J ($\times 10^{-7}$ cm^{-1})	0.609	0.753	0.731	Keenan et al.[5]	0.007	systematic
^{84}Kr−D^{79}Br(00^00) $\langle P_2(\cos\theta)\rangle$	0.696	0.656	0.600	Keenan et al.[5]	0.02	systematic
^{84}Kr−D^{79}Br(00^00) D_θ ($\times 10^{-6}$)	3.1	9.7	9.5	Keenan et al.[5]	0.6	statistical
[^{84}Kr−H^{79}Br(10^00) − ^{84}Kr−H^{79}Br(00^00)] − H^{79}Br(ν_1) (cm^{-1})	−4.79	−1.74	−1.74	present study[b]	0.01	approximation
^{84}Kr−H^{79}Br(10^00) B_0 ($\times 10^{-2}$ cm^{-1})	2.221	2.256	2.259	present study[b]	0.002	approximation
^{84}Kr−H^{79}Br(10^00) D_J ($\times 10^{-7}$ cm^{-1})	0.63	0.80	0.86	present study[b]	0.03	systematic
^{84}Kr−H^{79}Br(11^10) − ^{84}Kr−H^{79}Br (100) (cm^{-1})	45.24	32.55	32.56	present study[b]	0.03	approximation
^{84}Kr−H^{79}Br(11^10) B_0 ($\times 10^{-2}$ cm^{-1})	2.283	2.352	2.349	present study[b]	0.002	approximation
^{84}Kr−H^{79}Br(11^10) D_J ($\times 10^{-7}$ cm^{-1})	0.93	0.73	0.57	present study[b]	0.03	systematic
^{84}Kr−^{79}BrH(12^00) − ^{84}Kr−H^{79}Br (10^00) (cm^{-1})	29.02	35.82	35.82	present study[b]	0.04	approximation
^{84}Kr−^{79}BrH(12^00) B_0 ($\times 10^{-2}$ cm^{-1})	2.495	2.514	2.514	present study[b]	0.002	approximation
^{84}Kr−^{79}BrH(12^00) D_J ($\times 10^{-7}$ cm^{-1})	−1.5	2.3	2.1	present study[b]	0.1	systematic
G	127.1	2.4				

[a] Also given are the experimental data used in the fit with the estimated uncertainties in either the experimental data or in the calculation and the root-mean-square deviations from the experimental data of the two sets of predicted constants. [b] See Table 1. [c] The uncertainties used in the nonlinear least-squares procedure came from three sources: approximation (estimated uncertainties due to approximations in the calculation, usually taken to be 1 part in 1000), statistical (estimated experimental statistical uncertainties), and systematic (estimated experimental uncertainties due to systematic errors).

this parameter is an isotropic scaling factor that would not change the relative depths of the two potential minima, but only control the average depth of the potential. Therefore, lacking any currently available experimental data that concern the absolute well depth, we have not optimized this parameter. The average well depth is thus constrained to be the same as that determined in the pure ab initio calculation. The correlation matrix of the morphing parameters is given in Table 3. The corresponding values of the observables computed using the ab initio and morphed potentials are compared to the experimental data in Table 4. From Table 3, we see that the potential scaling parameters are fairly correlated. As noted previously, the values of these parameters are most strongly controlled by the values of $\langle P_2(\cos\theta)\rangle$ and the energy differences ^{84}Kr−H^{79}Br(11^10) − ^{84}Kr−H^{79}Br(10^00) and ^{84}Kr−^{79}BrH(12^00) − ^{84}Kr−H^{79}Br(10^00). Thus, there are four data points for four parameters. However, the values of $\langle P_2(\cos\theta)\rangle$ for the Kr−HBr and Kr−DBr isomers and the value of ^{84}Kr−H^{79}Br(11^10) − ^{84}Kr−H^{79}Br(10^00) are all giving information about the bending potential in the HB well and, thus, are not very independent, which leads to the high correlation between the potential scaling parameters. None of the other parameters are highly correlated.

The resulting interaction potentials are shown in Figure 4, and the corresponding uncertainties are given in Figure 5. The plots are given in Jacobi coordinates for the ^{84}Kr:H^{79}Br isotopomer, where R' is the distance from Kr to the center of mass of H^{79}Br and θ' is the angle ∠Kr−(center of mass of H^{79}Br)−H. θ' is defined such that $\theta' = 0°$ corresponds to the HB structure Kr−H−Br and $\theta' = 180°$ corresponds to the van der Waals (vdW) structure Kr−Br−H. On the ab initio potential ($\gamma = \infty$), the HB structure had $R'_{\text{min}} = 4.30$ Å and $V^{\text{int}} = -235$ cm^{-1}, and the vdW structure had $R'_{\text{min}} = 3.85$ Å and $V^{\text{int}} = -213$ cm^{-1}. Correspondingly, on the morphed potential ($\gamma = 10$), we found the HB minimum to be at $R'_{\text{min}} = 4.28$ Å with $V^{\text{int}} = -237$ cm^{-1} and the vdW minimum to be at $R'_{\text{min}} = 3.88$ Å with $V^{\text{int}} = -260$ cm^{-1}. Thus, the potential morphing changed the geometries by only a few hundredths of an angstrom; however, there was a more substantial change in the energies, with an almost 50 cm^{-1} reduction of the vdW minimum, relative to the HB minimum, going from the ab initio to the morphed potential.

In Figure 6, we give the probability density for the rovibrational wave functions of four states of the ^{84}Kr:H^{79}Br isotopomer. We can see that the ground state (00^00) is fairly well-localized in the HB well, and the state that corresponds to the vdW structure Kr−BrH (02^00) is a very compact wave function in the vdW well with a small amount of probability in the HB well. Finally, the π-bending state (01^10) is also primarily in the HB well, although it has been shifted away from the $\theta' = 0$ direction, because of the angular momentum about the intermolecular axis.

The difference between the morphed and ab initio results for the difference between the two minima can be analyzed in terms of the limited basis set and limited inclusion of correlation in

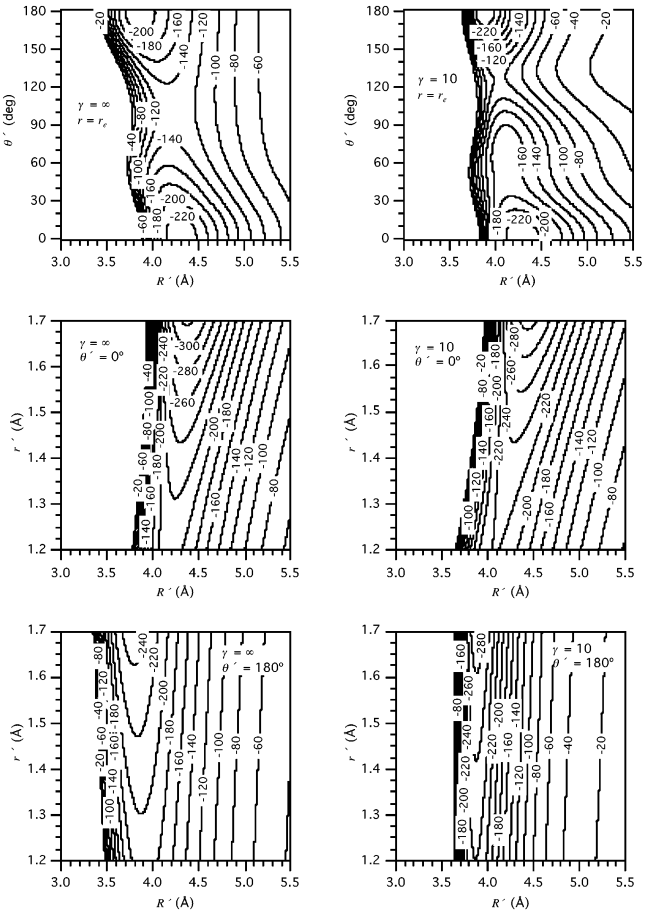

Figure 4. Comparison of the ab initio ($\gamma = \infty$) and morphed ($\gamma = 10$) interaction potentials of Kr:HBr. For each potential, three different cuts through the three-dimensional potential energy surface are given: $V^{int}(R',\theta',r = r_e)$, $V^{int}(R',\theta' = 0°,r)$, and $V^{int}(R',\theta' = 180°,r)$. All contours are given in units of cm^{-1}. Plots are given in Jacobi coordinates for the $^{84}Kr:H^{79}Br$ isotopomer. $\theta' = 0°$ corresponds to the HB structure Kr−H−Br and $\theta' = 180°$ corresponds to the vdW Kr−Br−H structure. For $\gamma = \infty$ and $\theta' = 0°$, $R'_{min} = 4.30$ Å and $V^{int} = -235$ cm^{-1}; for $\gamma = \infty$ and $\theta' = 180°$, $R'_{min} = 3.85$ Å and $V^{int} = -213$ cm^{-1}; for $\gamma = 10$ and $\theta' = 0°$, $R'_{min} = 4.28$ Å and $V^{int} = -237$ cm^{-1}; and for $\gamma = 10$ and $\theta' = 180°$, $R'_{min} = 3.88$ Å and $V^{int} = -260$ cm^{-1}.

the ab initio potential energy surface. We have examined how this energy difference changes as the basis set and correlation treatment improves. In Table 5, we give the results of additional ab initio calculations where we have systematically improved the basis set and extrapolated this to the complete basis set (CBS) limit, using an exponential extrapolation of the form[35]

$$A(n) = A_\infty + Be^{-(n-1)} + Ce^{-(n-1)^2}, \qquad (6)$$

where A is some computed property (i.e., D_e or R'_e), A_∞ is the estimated CBS limit of that property, and n is the order of the aug-pVnZ basis set used. The functional form given in eq 6 is then used to fit the results of either the $n = 2$ to $n = 5$ calculations or the $n = 3$ to $n = 5$ calculations. We have also considered the inclusion of additional correlation beyond that included in the MP2 calculation using the single and double excitation coupled cluster theory with perturbative treatment of triple excitations (CCSD(T)). All calculations were performed using the CP correction for the BSSE and with the H−Br bond length fixed at its equilibrium value of 1.4144 Å. The energy of the HB structure converges more rapidly with the size of the basis set than does the energy of the vdW structure. Even with the largest basis set used, aug-cc-pV5Z, the CP corrections are

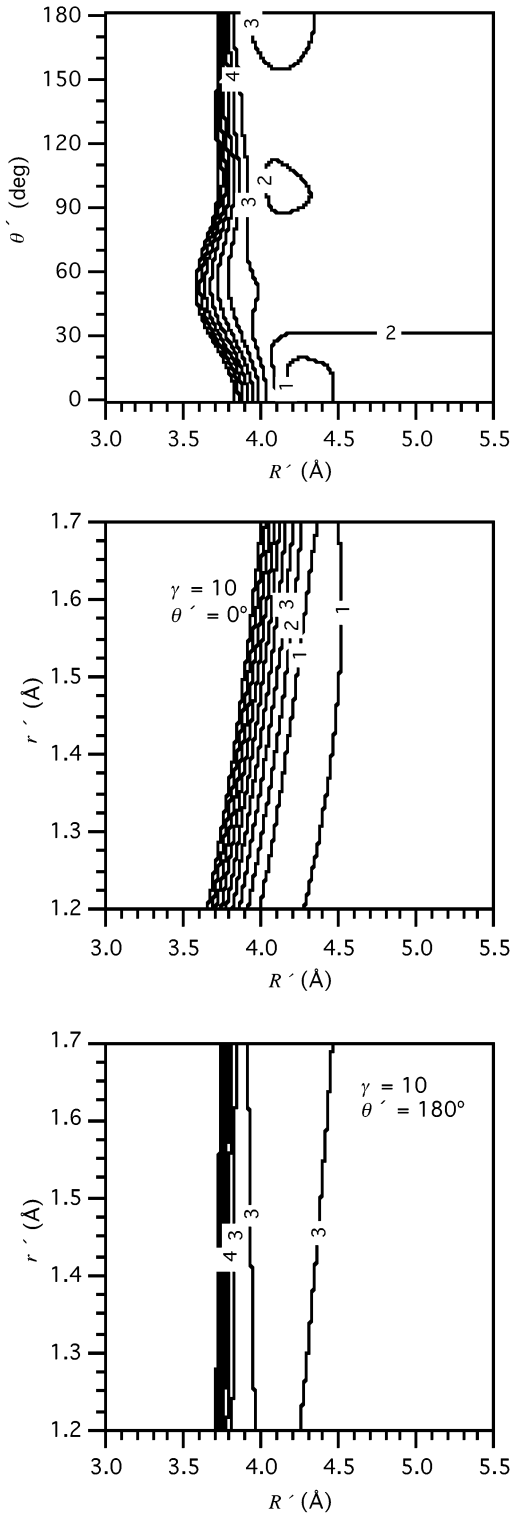

Figure 5. Estimate of the uncertainty in the morphed ($\gamma = 10$) potential for the same three cuts of the three-dimensional potential energy surface as shown in Figure 4. All contours are given in units of cm^{-1}. Plots are given in Jacobi coordinates for the $^{84}Kr:H^{79}Br$ isotopomer.

still quite large: 150.4 cm^{-1} for the HB structure and 112.3 cm^{-1} for the vdW structure in the CCSD(T) calculations. One would need to go to extremely large basis sets before the BSSE is small compared to the energy differences that we have considered here.[36] In addition, we have also examined the sensitivity of the energy difference between the two structures to the correlation of the core orbitals. We have computed the CCSD(T) energy using the aug-cc-pVQZ basis set and allowing

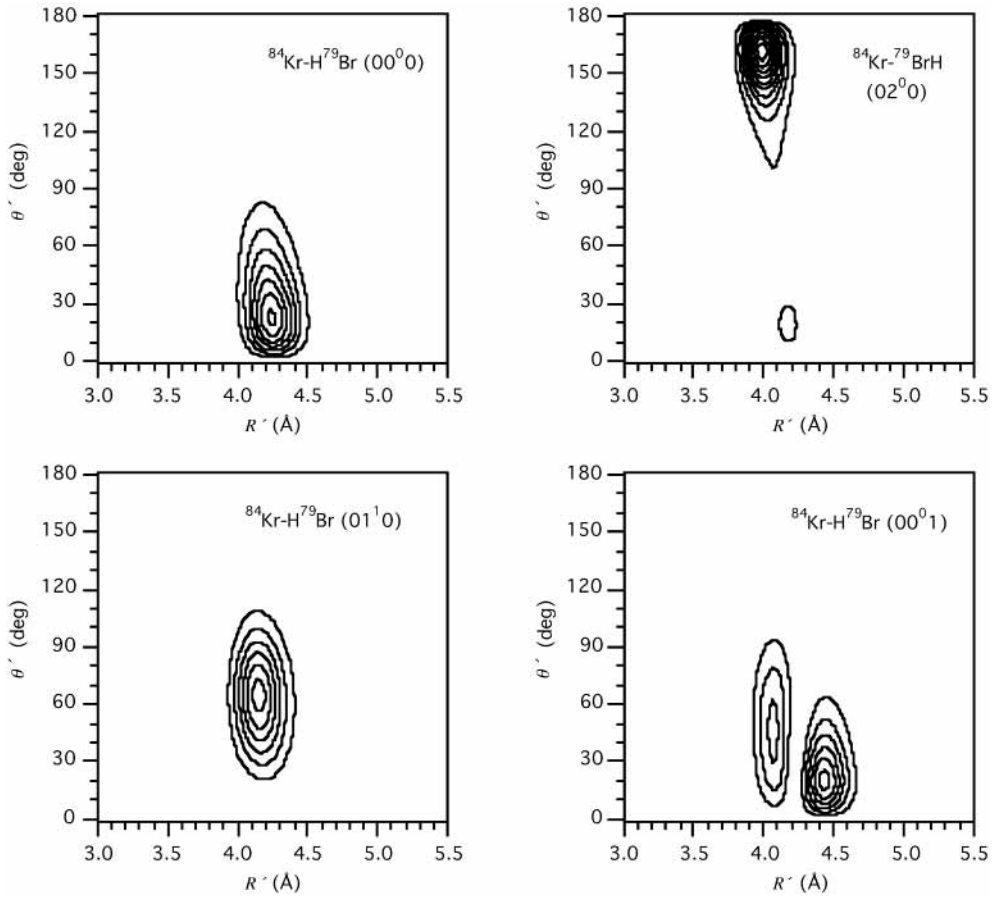

Figure 6. Probability density of the four lower rovibrational states of the ^{84}Kr:H^{79}Br isotopomer. Energies of these states and other spectroscopic constants are given in Table 6. Plots are given in Jacobi coordinates for the ^{84}Kr:H^{79}Br isotopomer.

TABLE 5: Values of D_e and R_e', Computed with the H−Br Bond Length Fixed at Its Experimental Value of 1.4144 Å

	Hydrogen-Bound		van der Waals		
calculation[a]	R_e' (Å)	D_e (cm^{-1})	R_e' (Å)	D_e (cm^{-1})	D_e (HB) − D_e (vdW) (cm^{-1})
MP2 $n = 2$	4.47	166.0	3.98	149.1	16.9
MP2 $n = 3$	4.30	235.8	3.85	213.0	22.8
MP2 $n = 4$	4.25	264.8	3.76	259.3	5.5
MP2 $n = 5$	4.24	275.1	3.75	273.5	1.5
MP2 CBS (3−5)	4.23	281.0	3.73	281.8	−0.8
MP2 CBS (2−5)	4.23	281.5	3.72	284.9	−3.4
CCSD(T) $n = 2$	4.55	132.5	4.08	105.9	26.5
CCSD(T) $n = 3$	4.38	185.2	3.94	157.5	27.7
CCSD(T) $n = 4$	4.34	206.3	3.85	193.4	12.9
CCSD(T) $n = 5$	4.33	211.3	3.83	202.8	8.5
CCSD(T) CBS (3−5)	4.32	214.2	3.83	208.3	5.9
CCSD(T) CBS (2−5)	4.32	216.3	3.81	211.9	4.5
morphed ($\gamma = 10$)	4.27	236.9	3.88	259.4	−22.5

[a] The value of n indicates which aug-cc-pVnZ basis set is used.

the 3s and 3p orbitals of Kr and Br to be correlated. Inclusion of this additional correlation leads to a reduction of the vdW well by 1.1 cm^{-1} relative to the HB well, when the optimized aug-cc-pVQZ CCSD(T) geometries given in Table 5 were used. Furthermore, we have considered the effect of adding a second set of diffuse functions by performing a CCSD(T) calculation using the d-aug-cc-pVQZ basis set.[24] This leads to an additional reduction of the vdW well of 4.8 cm^{-1}, relative to the HB well. Thus, combining the CBS CCSD(T) results in Table 5 and these two estimates of remaining correlation and basis sets effects leads to an ab initio estimate of D_e(HB) − D_e(vdW) = −1 cm^{-1}, which is ∼20 cm^{-1} above the value observed in the morphed potential of D_e(HB) − D_e(vdW) = −23 ± 3 cm^{-1}. As previously observed in calculations on the related Ar:HF[37] and Ar:HCl[35] systems, the energy in the vdW structure converges more slowly than does the energy in the HB structure, with respect to increasing basis set size. Thus, the remaining difference may by due a poor CBS extrapolation based on basis sets that are not large enough. A further possible source of disagreement may be the neglect of relativistic effects in the present calculations.

In Table 6, we give predictions obtained from the morphed potential for some transitions that have not yet been observed and values for $\langle P_1(\cos\theta)\rangle$ for all states considered here. We can see that the values of ΔE for the lower ($v_1 = 0$) and upper ($v_1 = 1$) states are all within 1 cm^{-1} of each other. The values

TABLE 6: Values of Selected Spectroscopic Constants Predicted from the Morphed Potential for the ^{84}Kr:H^{79}Br Isotopomer

state	ΔE^a (cm^{-1})	B_0 ($\times 10^{-2}$ cm^{-1})	D_J ($\times 10^{-7}$ cm^{-1})	$\langle P_1(\cos\theta)\rangle$	$\langle P_2(\cos\theta)\rangle$
(00^00)	0.00	2.285	0.809	0.741	0.432
(00^01)	23.36	2.246	1.043	0.679	0.385
(02^00)	36.17	2.509	1.758	−0.585	0.556
(01^10)	31.53	2.365	0.718	0.384	−0.100
(10^00)	−1.74[b]	2.256	0.800	0.763	0.469
(10^01)	23.08	2.229	1.112	0.688	0.397
(12^00)	35.82	2.514	2.261	−0.618	0.586
(11^10)	32.55	2.352	0.729	0.392	−0.094

[a] $\Delta E = E(\upsilon_1, \upsilon_2^l, \upsilon_3) - E(\upsilon_1, 0^0, 0)$. [b] In this case, $\Delta E = [E(1, 0^0, 0) - E(0, 0^0, 0)] - \upsilon(H^{79}Br)$.

of $\langle P_1(\cos\theta)\rangle$ for the lower states are consistent with the probability densities shown in Figure 6. In particular, we can see that in the (02^00) state the value of $\langle P_1(\cos\theta)\rangle$ is somewhat smaller in magnitude than for the corresponding (00^00) state, which is a reflection of the fact that the (02^00) state has some probability in both wells. Also, we can see the shift in probability away from the linear configuration in the (01^10) state in the small value of $\langle P_1(\cos\theta)\rangle$, which agrees with the position of the probability for this state, observed in Figure 6.

Discussion

It has been an oft-held tenet of molecular structure that the atomic arrangements for molecular species in the ground state and at equilibrium have the same isomeric configuration. Indeed, this has been widely assumed in procedures for estimating equilibrium structures that have been experimentally determined from spectroscopic data.[20,38] In almost all instances, this assumption is justifiable and leads to relatively small discrepancies in equilibrium bond lengths and angles. However, for a restricted number of molecular species, it is possible that the previously discussed assumption is not valid. Weakly bound complexes that involve a low barrier that can also involve interconversions between nonequivalent isomeric states and large amplitude anharmonic vibrations are candidates for which the discussed implicit assumption may not be justified.[2−4] In effect, zero-point energy effects can result in the ground state and equilibrium structures being significantly different. In an extensive recent study of Ar:HBr using morphing procedures,[1,2] we observed that the ground vibrational state had the Ar−HBr atomic arrangement, in contrast to the global energy minimum, which had the Ar−BrH structure. This conclusion was considered significant, based on an unequivocal arrangement of the lowest vibrational energy states established using an extensive spectroscopic database[34] and the estimated accuracy of the determined morphed potential.[1,2]

Within the context of these investigations, it seems to be worthwhile to consider whether other systems could be demonstrated to have similar characteristics. In the current investigation, we have also used potential morphing to determine the equilibrium structure of Kr:HBr and compare this result with its experimentally determined ground-state structure.[5]

The results for Kr:HBr are comparable and, in many respects, similar to the results obtained from an investigation of Ar:HBr, in which the corresponding value between the minima of the potentials associated with the two isomeric forms was 25 ± 3 cm^{-1}.[2] Thus, the substitution of the more easily polarizable Kr atom for Ar has resulted in a global minimum with a vdW Kr−Br structure that has a collinear R'_{min} value of 3.88 Å, which contrasts with the determined Kr−HBr ground state. Thus, the Kr:HBr complex is also proposed as a molecular species in which its ground-state atomic arrangement is differently bound from its equilibrium structure. It is pertinent to note that this value of R is comparable to the sum of the van der Waals radii of Kr and Br.[39]

The comparison of the ab initio results and the morphed potential in this study shows that the level of agreement is somewhat worse than the ± 3 cm^{-1} difference found between ab initio and experimentally derived potentials in the Ar:HCl system for the difference in energy of the HB and vdW wells in that system.[35] This would suggest that the ab initio techniques commonly used to study intermolecular interactions may not be as accurate for systems with heavier atoms, such as those in the present study.

Conclusions

We have recorded the infrared spectra of the ν_1, $\nu_1 + \nu_2^1$, and $\nu_1 + 2\nu_2^0$ vibrations in ^{84}Kr:H^{79}Br and ^{84}KrH^{81}Br isotopomers and combined this with a previously recorded pulsed-nozzle Fourier transform (FT) microwave in a supersonic slit-jet expansion. Such a combination of data thus makes available experimental information that has been used as a basis for a comparison with ab initio calculations and has been used to model the rovibrational tunneling dynamics of ^{84}Kr:H^{79}Br. The morphed potential energy surface obtained in this study has a global minimum at the van der Waals (vdW) Kr−BrH structure but with a ground rovibrational state that is localized in the minimum corresponding to the hydrogen-bound (HB) Kr−HBr structure. The vdW structure was 23 ± 3 cm^{-1} lower in energy than the HB structure, which was indicative that the calculated energy difference between the HB and vdW potentials are statistically significant, given the estimated uncertainties of the experimental data used in the morphing procedure.

Acknowledgment. This material is based on work supported by the National Science Foundation (under Grant No. CHE-0200972). J.W.B. thanks the Welch Foundation for financial support (under Grant No. A-747). The support of the Texas A&M University Supercomputing Facility is also acknowledged.

References and Notes

(1) Castillo-Chará, J.; Lucchese, R. R.; Bevan, J. W. *J. Chem. Phys.* **2001**, *115*, 899.

(2) Belov, S. P.; McElmurry, B. A.; Lucchese, R. R.; Bevan, J. W.; Leonov, I. *Chem. Phys. Lett.* **2003**, *370*, 528.

(3) Huang, S. S.; Bieler, C. R.; Janda, K. C.; Tao, F.-M.; Klemperer, W.; Casavecchia, P.; Volpi, G. G.; Halberstadt, N. *J. Chem. Phys.* **1995**, *102*, 8846.

(4) Liu, K.; Brown, M. G.; Carter, C.; Saykally, R. J.; Gregory, J. K.; Clary, D. C. *Nature* **1996**, *381*, 501.

(5) Keenan, M. R.; Campbell, E. J.; Balle, T. J.; Buxton, L. W.; Minton, T. K.; Soper, P. D.; Flygare, W. H. *J. Chem. Phys.* **1980**, *72*, 3070.

(6) Hutson, J. M. *J. Chem. Phys.* **1989**, *91*, 4455.

(7) Bulanin, M. O.; Bulychev, V. P. *Opt. Spectrosc.* **1993**, *75*, 436.

(8) Kisiel, Z. *J. Mol. Spectrosc.* **2003**, *218*, 58.

(9) Watson, J. K. G. *Mol. Phys.* **2002**, *100*, 47.

(10) Meuwly, M.; Hutson, J. M. *J. Chem. Phys.* **1999**, *110*, 8338.

(11) McIntosh, A. L.; Wang, Z.; Castillo-Chara, J.; Lucchese, R. R.; Bevan, J. W.; Suenram, R. D.; Legon, A. C. *J. Chem. Phys.* **1999**, *111*, 5764.

(12) McIntosh, A.; Gallegos, A. M.; Lucchese, R. R.; Bevan, J. W. *J. Chem. Phys.* **1997**, *107*, 8327.

(13) McIntosh, A.; Lin, P.; Lucchese, R. R.; Bevan, J. W.; Brugh, D. J.; Suenram, R. D. *Chem. Phys. Lett.* **2000**, *331*, 95.

(14) Lin, P.; Jabs, W.; Lucchese, R. R.; Bevan, J. W.; Brugh, D. J.; Suenram, R. D. *Chem. Phys. Lett.* **2002**, *356*, 101.

(15) Wang, Z. C.; Eliades, M.; Carron, K.; Bevan, J. W. *Rev. Sci. Instrum.* **1991**, *62*, 21.

(16) McIntosh, A. L.; Wang, Z.; Lucchese, R. R.; Bevan, J. W. High-Frequency Wavelength Modulation CW Slit Jet Diode Laser Spectrometer for Characterizing Ground State Intermolecular Hydrogen Bonded Vibrations. *Infrared Phys. Technol.*, in press.

(17) Hutson, J. M. *J. Chem. Phys.* **1992**, *96*, 6752.

(18) Hutson, J. M. *J. Phys. Chem.* **1992**, *96*, 4237.

(19) Busarow, K. L.; Blake, G. A.; Loughlin, K. B.; Saykally, R. J. *Chem. Phys. Lett.* **1987**, *141*, 289.

(20) Gordy, W.; Cook, R. L. *Microwave Molecular Spectra*, 3rd Ed.; Techniques of Chemistry XVIII; Wiley: New York, 1984.

(21) Guelachvilli, G.; Rao, K. N. *Handbook of Infrared Standards*; Academic Press: New York, 1986.

(22) Huber, K. P.; Herzberg, G. *Molecular Spectra and Molecular Structure IV. Constants of Diatomic Molecules*; Van Nostrand Reinhold: New York, 1979.

(23) (a) Dunning, T. H., Jr. *J. Chem. Phys.* **1989**, *90*, 1007. (b) Kendall, R. A.; Dunning, T. H., Jr. *J. Chem. Phys.* **1992**, *96*, 6796. (c) Wilson, A. K.; Woon, D. E.; Peterson, K. A.; Dunning, T. H., Jr. *J. Chem. Phys.* **1999**, *110*, 7667.

(24) Woon, D. E.; Dunning, T. H., Jr. *J. Chem. Phys.* **1994**, *100*, 2975.

(25) Boys, S. F.; Bernardi, F. *Mol. Phys.* **1970**, *19*, 553.

(26) Frisch, M. J.; Trucks, G. W.; Schlegel, H. B.; Scuseria, G. E.; Robb, M. A.; Cheeseman, J. R.; Zakrzewski, V. G.; Montgomery, J. A., Jr.; Stratmann, R. E.; Burant, J. C.; Dapprich, S.; Millam, J. M.; Daniels, A. D.; Kudin, K. N.; Strain, M. C.; Farkas, O.; Tomasi, J.; Barone, V.; Cossi, M.; Cammi, R.; Mennucci, B.; Pomelli, C.; Adamo, C.; Clifford, S.; Ochterski, J.; Petersson, G. A.; Ayala, P. Y.; Cui, Q.; Morokuma, K.; Rega, N.; Salvador, P.; Dannenberg, J. J.; Malick, D. K.; Rabuck, A. D.; Raghavachari, K.; Foresman, J. B.; Cioslowski, J.; Ortiz, J. V.; Baboul, A. G.; Stefanov, B. B.; Liu, G.; Liashenko, A.; Piskorz, P.; Komaromi, I.; Gomperts, R.; Martin, R. L.; Fox, D. J.; Keith, T.; Al-Laham, M. A.; Peng, C. Y.; Nanayakkara, A.; Challacombe, M.; Gill, P. M. W.; Johnson, B.; Chen, W.; Wong, M. W.; Andres, J. L.; Gonzalez, C.; Head-Gordon, M.; Replogle, E. S.; Pople, J. A. *Gaussian 98*, Revision A.11.3; Gaussian, Inc.: Pittsburgh, PA, 2002.

(27) Amos, R. D.; Bernhardsson, A.; Berning, A.; Celani, P.; Cooper, D. L.; Deegan, M. J. O.; Dobbyn, A. J.; Eckert, F.; Hampel, C.; Hetzer, G.; Knowles, P. J.; Korona, T.; Lindh, R.; Lloyd, A. W.; McNicholas, S. J.; Manby, F. R.; Meyer, W.; Mura, M. E.; Nicklass, A.; Palmieri, P.; Pitzer, R.; Rauhut, G.; Schütz, M.; Schumann, U.; Stoll, H.; Stone, A. J.; Tarroni, R.; Thorsteinsson, T.; Werner, H.-J. *MOLPRO*, Version 2002.1, Birmingham, U.K., 2002. (MOLPRO is a package of ab initio programs designed by H.-J.Werner and P. J. Knowles.)

(28) Ho, T. S.; Rabitz, H. *J. Chem. Phys.* **1996**, *104*, 2584.

(29) Han, J.; McIntosh, A. L.; Wang, Z.; Lucchese, R. R.; Bevan, J. W. *Chem. Phys. Lett.* **1997**, *265*, 209.

(30) Quinones, A.; Bandarage, G.; Bevan, J. W.; Lucchese, R. R. *J. Chem. Phys.* **1992**, *97*, 2209.

(31) De Lucia, F. C.; Helminger, P.; Gordy, W. *Phys. Rev. A* **1971**, *3*, 1849.

(32) Rank, D. H.; Fink, U.; Wiggins, T. A. *J. Mol. Spectrosc.* **1965**, *18*, 170.

(33) Press: W. H.; Flannery, B. P.; Teukolsky, S. A.; Vetterling, W. T. *Numerical Recipes. The Art of Scientific Computing*; Cambridge University Press: Cambridge, U.K., 1986.

(34) Han, J.; McIntosh, A. L.; Hartz, C. L.; Lucchese, R. R.; Bevan, J. W. *Chem. Phys. Lett.* **1997**, *268*, 209.

(35) Woon, D. E.; Peterson, K. A.; Dunning, T. H., Jr. *J. Chem. Phys.* **1998**, *109*, 2233.

(36) Stålring, J.; Schutz, M.; Lindh, R.; Karlstrom, G.; Widmark, P.-O. *Mol. Phys.* **2002**, *100*, 3389.

(37) van Mourik, T.; Dunning, T. H., Jr. *J. Chem. Phys.* **1997**, *107*, 2451.

(38) Harmony, M. D. *Acc. Chem. Res.* **1992**, *25*, 321.

(39) Cotton, F. A.; Wilkinson, G. *Advanced Inorganic Chemistry, A Comprehensive Text*, 3rd ed.; Interscience: New York, 1972.